The Astrophysical Journal, 711:796–807, 2010 March 10 doi:10.1088/0004-637X/711/2/796

AN ASSESSMENT OF THE ENERGY BUDGETS OF LOW-IONIZATION NUCLEAR EMISSION REGIONS

Michael Eracleous[1,2,3], Jason A. Hwang[1,3], and Hélène M. L. G. Flohic[1,4]
[1] Department of Astronomy and Astrophysics, The Pennsylvania State University, 525 Davey Lab, University Park, PA 16802, USA
[2] Center for Gravitational Wave Physics, The Pennsylvania State University, 104 Davey Lab, University Park, PA 16802, USA
[3] Department of Physics & Astronomy, Northwestern University, 2131 Tech Drive, Evanston, IL 60208, USA
[4] Department of Physics and Astronomy, University of California, 4129 Frederick Reines Hall, Irvine, CA 92697, USA
Received 2007 September 19; accepted 2010 January 22; published 2010 February 18

ABSTRACT

Using the spectral energy distributions (SEDs) of the weak active galactic nuclei (AGNs) in 35 low-ionization nuclear emission regions (LINERs) presented in a companion paper, we assess whether photoionization by the weak AGN can power the emission-line luminosities measured through the large (few-arcsecond) apertures used in ground-based spectroscopic surveys. Spectra taken through such apertures are used to define LINERs as a class and constrain non-stellar photoionization models for LINERs. Therefore, our energy budget test is a self-consistency check of the idea that the observed emission lines are powered by an AGN. We determine the ionizing luminosities and photon rates by integrating the observed SEDs and by scaling a template SED. We find that even if all ionizing photons are absorbed by the line-emitting gas, more than half of the LINERs in this sample suffer from a deficit of ionizing photons. In 1/3 of LINERs the deficit is severe. If only 10% of the ionizing photons are absorbed by the gas, there is an ionizing photon deficit in 85% of LINERs. We disfavor the possibility that additional electromagnetic power, either obscured or emitted in the unobservable far-UV band, is available from the AGN. Therefore, we consider other power sources such as mechanical heating by compact jets from the AGN and photoionization by either young or old stars. Photoionization by young stars may be important in a small fraction of cases. Mechanical heating can provide enough power in most cases but it is not clear how this power would be transferred to the emission-line gas. Photoionization by post asymptotic giant branch stars is an important power source; it provides more ionizing photons than the AGN in more than half of the LINERs and enough ionizing photons to power the emission lines in 1/3 of the LINERs. It appears likely that the emission-line spectra of LINERs obtained from the ground include the sum of emission from different regions where different power sources dominate.

Key words: galaxies: active – galaxies: nuclei – X-rays: galaxies

1. INTRODUCTION

The nature of low-ionization nuclear emission regions (LINERs) has been the subject of considerable debate since their identification as a class by Heckman (1980). Their defining characteristics are the relative intensities of their oxygen emission lines, namely [O II] λ3727/[O III] λ5007 > 1 and [O I] λ6300/[O III] λ5007 > 1/3. They are found in approximately 50% of nearby galaxies (Ho et al. 1997a), which suggests that they are an important component of galactic nuclei in the local universe. The emission lines could be powered by (1) photoionization by an accreting supermassive black hole, i.e., a "little monster" or an active galactic nucleus (AGN; e.g., Halpern & Steiner 1983; Ferland & Netzer 1983), (2) hot stars (either young stars in a compact starburst or the hot, exposed cores of evolved stars; e.g., Terlevich & Melnick 1985; Filippenko & Terlevich 1992; Shields 1992; Barth & Shields 2000; Binette et al. 1994), or (3) shocks (e.g., Heckman 1980; Dopita et al. 1996, and references therein). Recent radio, UV, and X-ray surveys at high spatial resolution and UV variability studies find "little monsters" in the majority of LINERs observed (e.g., Nagar et al. 2002, 2005; Filho et al. 2004, 2006; Barth et al. 1998; Maoz et al. 1995; Ho et al. 2001; Terashima & Wilson 2003; Dudik et al. 2005; Flohic et al. 2006; González-Martín et al. 2006; Maoz et al. 2005). Thus, LINERs are potentially the largest subset of AGNs, tracing the AGN population at the lowest luminosities and providing us an opportunity to study the properties of the accretion flow in these low-luminosity AGNs.

However, a separate and equally important question remains unanswered: how important is photoionization by the "little monsters" in powering the emission-line luminosity measured in the spectra of these objects? If "little monsters" are not significant or universal power sources, then we must find alternate sources of power and understand their relation, if any, to the "little monster." LINERs and related objects are typically identified in spectroscopic surveys using telescopes on the ground. Thus, the spectra are taken through apertures whose characteristic angular size is a few arcseconds. A very important survey is that of Ho et al. (1997a, see also references therein), which has systematically identified a large number of LINERs among nearby, bright galaxies in the northern sky. The spectra for this survey were taken through a 2″ × 4″ slit, corresponding to a physical dimension of a few hundred parsec at the distances of the target galaxies. These spectra provide some of the main observational constraints for models that attempt to explain LINERs, specifically, photoionization models assuming that the ionizing photons come from a "little monster." Therefore, the question we address here is whether the "little monsters" can provide enough power and enough ionizing photons to account for the emission-line luminosity observed through apertures of a few arcseconds. This comparison is appropriate because these are the same apertures through which the defining line ratios of LINERs and related objects are measured. In other words, our goal is to carry out a self-consistency test of non-stellar photoionization models since these models should not only explain the line ratios but also the line luminosities.

The question of the energy budget of LINERs has been tackled by a number of authors in the recent literature (see the recent review by Ho 2008). In their evaluation of the excitation mechanism in a sample of 13 LINERs, Ho et al. (1993) found a deficit of ionizing photons from the AGN, even though the corresponding photoionization models were successful in

reproducing the relative intensities of the optical emission lines. They proposed that either the AGN provides more ionizing photons than they assumed (which are either extinguished or unobservable) or that some other power source makes up the deficit. Maoz et al. (1995), using their near-UV photometry of a sample of five UV-bright LINERs and an assumed shape for the spectral energy distribution (SED), found that the AGN could provide enough photons to power the observed emission lines. In a follow-up study employing UV spectra of seven objects, Maoz et al. (1998) re-evaluated the energy budgets of LINERs using both AGN and starburst models for the SED. They concluded that there is indeed a deficit of ionizing photons for about half of the objects in their sample, specifically those with AGN-like UV spectra. They suggested that extreme-UV/soft-X-ray photons emitted by the AGN provide the missing power. More recently, Flohic et al. (2006) assessed the budget of ionizing photons from the AGN in a sample of 19 LINERs observed in the X-ray band with *Chandra*. They extrapolated the observed X-ray power law to the Lyman limit and found that the AGN could not provide the requisite number of ionizing photons. They proposed that either photons from post asymptotic giant branch (AGB) stars from an intermediate-age stellar population or mechanical power from a jet emanating from the AGN make up the deficit.

In this paper, we re-evaluate the electromagnetic energy budgets of the "little monsters" in LINERs using an X-ray-selected sample of 35 objects with published data. In a companion paper (Eracleous et al. 2010, hereafter Paper I), we put together the SEDs of these objects and use a subset of those data to address the question of whether *photoionization from the weak AGN* can power the (narrow) emission-line luminosity observed through a $2'' \times 4''$ aperture in the survey of Ho et al. (1997b). In Section 2, we present the sample of galaxies and their basic properties, and we briefly summarize how we collected the data (details are given in Paper I) and how we applied extinction corrections. In Section 3, we describe how we integrated the SEDs to compute the ionizing luminosity and rate of ionizing photons from the AGN. In Section 4, we compare the ionizing luminosities and photon rates with the emission-line luminosity and photon rate, and we find a general deficit of ionizing photons. We discuss possible ways of balancing the budget in Section 5 by asking whether our estimates have missed part of the ionizing photon output of the AGN and by considering other processes that may contribute to the excitation of the nebula.

2. SAMPLE, SPECTRAL ENERGY DISTRIBUTIONS, AND REDDENING CORRECTIONS

Our sample of LINERs consists of 35 relatively nearby objects (all but one are at distances less than 40 Mpc) spanning all host morphological types and with a fairly representative distribution of LINER types. These are listed in Table 1 along with their basic properties including LINER types and nuclear Hα luminosities from Ho et al. (1997b). The Hα luminosities were measured through a $2'' \times 4''$ slit (see Ho et al. 1995, 1997b) and have uncertainties of 10%–30% in 27 objects, 30%–50% in one object (NGC 3608), and 100% in one object (NGC 3379). In one other object (NGC 4494), the quoted Hα luminosity is a "3σ" upper limit, while in the five remaining objects (NGC 2681, NGC 3031, NGC 4125, NGC 4736, and NGC 5055) the Hα luminosities are lower limits because the observations were made under non-photometric conditions. In Figure 1, we compare the distribution of Hα luminosities among the objects in our sample with that of similar objects in the Ho et al. (1997b) "parent" sample (i.e., LINERs with and without broad lines and "transition objects"). As this figure shows, our objects span the entire range of luminosities of the Ho et al. (1997b) parent sample, although high-luminosity objects are somewhat over-represented.

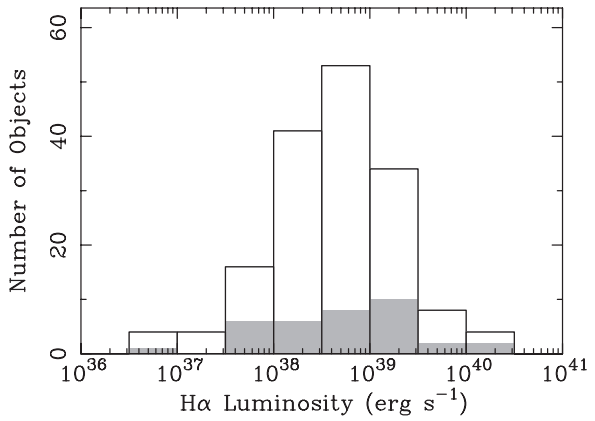

Figure 1. Distribution of Hα luminosities of objects in our sample, compared to that of objects in the Ho et al. (1997b) "parent" sample. Included in this histogram are LINERs with and without broad emission lines as well as "transition objects." The open bins show the distribution of Hα luminosities of all 164 objects in the Ho et al. (1997b) sample plus NGC 1097 and NGC 1553, while the shaded bins identify the subset of 35 objects included in our sample.

The sample galaxies were observed in the X-ray band with the *Chandra* X-Ray Observatory with moderately long exposure times. In 24 objects, the X-ray emission from a weak AGN was detected by *Chandra*, while for the remaining 11 objects an upper limit was obtained. We used data from the literature to construct the spectral energy distributions (SEDs) of these weak AGNs from the radio to the X-ray bands, which we present in Paper I along with derived quantities such as the bolometric luminosity, the Eddington ratio, and the optical-to-X-ray spectral index, α_{ox}.[5] Included in Paper I are also references to the sources of the data as well as an extensive discussion of relevant caveats. The 2–10 keV X-ray luminosities of the detected AGNs are between 1.7×10^{38} and 2.6×10^{41} erg s^{-1}, while the undetected AGNs have $L_{2-10\,\mathrm{keV}} < 1.2 \times 10^{39}$ erg s^{-1}. Their bolometric luminosities were derived by integrating the observed SED in a small fraction of objects or by scaling the X-ray luminosity for the majority of objects. Detected AGNs in this sample have 1.2×10^{38} erg s^{-1} $< L_{\mathrm{bol}} < 3.3 \times 10^{43}$ erg s^{-1} while the undetected objects have $L_{\mathrm{bol}} < 1.1 \times 10^{41}$ erg s^{-1} (see the detailed discussion in Section 4.1 of Paper I). Using black hole masses obtained from the stellar velocity dispersion in the host galaxies, we estimated the Eddington ratios (defined as the ratio of the bolometric luminosity to the Eddington luminosity; see Sections 2 and 4.1 of Paper I). We find that $3 \times 10^{-8} < \mathcal{R}_{\mathrm{Edd}} < 4 \times 10^{-4}$ for X-ray-detected AGNs, while undetected AGNs have $\mathcal{R}_{\mathrm{Edd}} < 2 \times 10^{-5}$ (see histogram in Figure 5 of Paper I).

Here we are primarily interested in the ionizing portion of the SED at $E > 1$ Ry. To define the SED at these energies we relied on UV photometry and spectroscopy of the nuclei carried out with the *Hubble Space Telescope* (*HST*) and X-ray observations carried out with *Chandra* (see references in Paper I). High spatial resolution in the UV and X-ray bands is

[5] The optical-to-X-ray spectral index is the exponent of a power law connecting the monochromatic luminosity densities at 2500 Å and 2 keV. If $L_\nu \propto \nu^{-\alpha_{ox}}$, α_{ox} is given by $\alpha_{ox} = 1 + 0.384 \log\left[(\nu L_\nu)_{2500\,\text{Å}}/(\nu L_\nu)_{2\,\mathrm{keV}}\right]$.

Table 1
Sample of LINERs and Their Properties

Galaxy	LINER		Measured SED		Quasar SED		
	Type[a]	$\log L_{H\alpha}$[a,b]	$\log L_i$[b]	$\log Q_i$[b]	$\log L_i$[b]	$\log Q_i$[b]	$\log Q_{\star,m_{44}}$[b,d]
(1)	(2)	(3)	(4)	(5)	(6)	(7)	(8)
NGC 0266	L1	39.30	< 41.81	< 51.59	41.86	52.01	50.99
NGC 0404	L2	37.63	38.94	49.37	37.57	47.72	48.69
NGC 1097	L1	38.72	41.52	51.43	41.62	51.77	...
NGC 1553	L2/T2	39.30	40.99	50.72	40.92	51.07	...
NGC 2681	L1	> 38.83	< 39.35	< 49.52	39.24	49.39	...
NGC 3031 (M81)	S1.5/L1	> 38.46	40.97	50.55	41.26	51.41	...
NGC 3169	L2	39.02	< 42.80	< 52.98	42.03	52.18	50.45
NGC 3226	L1	38.93	< 41.90	< 52.09	41.68	51.83	50.18
NGC 3379 (M105)	L2/T2	37.94	< 38.25	< 48.37	38.21	48.36	50.13
NGC 3507	L2	39.39	< 38.61	< 48.74	< 38.58	< 48.73	50.32
NGC 3607	L2	38.93	< 38.34	< 47.42	< 38.68	< 48.83	50.44
NGC 3608	L2/S2	38.28	< 39.79	< 49.92	< 39.76	< 49.91	50.64
NGC 3628	T2	36.87	< 37.72	< 47.84	< 37.68	< 47.83	48.03
NGC 3998	L1	40.00	42.36	52.40	42.40	52.55	50.87
NGC 4111	L2	39.40	< 40.30	< 49.90	< 40.54	< 50.69	50.74
NGC 4125	T2	> 38.96	< 39.75	< 49.87	< 39.72	< 49.87	...
NGC 4143	L1	38.69	< 41.02	< 51.10	41.01	51.17	50.41
NGC 4261 (3C 270)	L2	39.35	< 42.08	< 52.13	42.00	52.15	50.83
NGC 4278	L1	39.17	< 40.95	< 51.01	40.94	51.09	50.11
NGC 4314	L2	38.45	< 39.58	< 50.03	< 38.47	< 48.62	49.84
NGC 4374 (M84, 3C 272.1)	L2	38.89	40.31	50.05	40.53	50.68	50.33
NGC 4438	L1	39.37	< 39.77	< 49.23	< 40.06	< 50.21	49.97
NGC 4457	L2	39.57	< 40.07	< 50.21	39.99	50.14	50.83
NGC 4486 (M87, 3C 274)	L2	39.44	41.34	51.51	41.18	51.33	50.07
NGC 4494	L2	37.54	< 39.99	< 50.11	39.95	50.10	50.03
NGC 4548 (M91)	L2	38.46	< 40.41	< 49.50	40.72	50.87	49.88
NGC 4552 (M89)	T2	38.52	40.36	50.20	40.40	50.55	50.44
NGC 4579 (M58)	L1	39.44	41.91	51.26	42.23	52.38	50.37
NGC 4594 (M104)	L2	< 39.70	41.42	51.67	40.86	51.01	50.94
NGC 4636	L1	38.27	< 39.57	< 49.34	< 39.77	< 49.92	49.95
NGC 4736 (M94)	L2	> 37.75	39.72	49.71	39.76	49.91	...
NGC 5055 (M63)	T2	> 37.91	41.81	52.34	39.28	49.43	...
NGC 5866	T2	38.01	< 39.18	< 48.55	< 39.48	< 49.63	49.71
NGC 6500	L2	40.31	41.92	52.25	40.71	50.86	50.68
NGC 7331	T2	38.49	< 38.43	< 48.41	< 38.52	< 48.67	50.21

Notes.
[a] The LINER types and Hα line luminosities (measured through a $2'' \times 4''$ aperture) were taken from Ho et al. (1997b), with the exception of NGC 1097 and NGC 1553. The LINER types for these two galaxies were taken from Phillips et al. (1984, 1986), respectively. The emission-line luminosity of NGC 1097 was taken from Storchi-Bergmann et al. (1993), while that of NGC 1553 was taken from Phillips et al. (1986). L1: LINER with a broad Hα line, L2: LINER without a broad Hα line, T2: intermediate emission-line ratios between LINER and H II region, S: Seyfert, combinations indicate intermediate line ratios between two classes. The uncertainty on the Hα luminosity is 10%–30%, with the exception of NGC 3608 (30%–50%) and NGC 3379 (100%). In the case of NGC 4494, we list a "3σ" upper limit on the Hα luminosity. All upper limits on the Hα luminosity are the result of non-photometric sky conditions.
[b] The luminosities are measured in erg $s^{-1}$and the photon rates in s^{-1}.
[c] $\mathcal{R}_{Edd}$ is the Eddington ratio, defined as the ratio of the bolometric luminosity to the Eddington luminosity.
[d] The ionizing photon rate from post-AGB stars in the old stellar population. It is estimated from the spectroscopic *B* magnitude reported by Ho et al. (1997b) after converting it to a standard *B* magnitude and using the prescription of Binette et al. (1994). See details and discussion in Section 5 of the text.

essential in order to separate the AGN from discrete and diffuse sources in its immediate vicinity. From the UV observations we have obtained the monochromatic luminosity density at 2500 Å for 19 objects. We have used UV variability information (from Maoz et al. 2005) and UV spectra (primarily from Maoz et al. 1998) to separate "little monsters" from compact starbursts. By studying the distribution of α_{ox} of these two types of nuclei in Paper I, we found that "little monsters" always have $\alpha_{ox} < 1.4$. Adopting $\alpha_{ox} < 1.5$, we derived a *generous* upper limit for the 2500 Å fluxes of AGNs in our sample that were observed in the X-ray, but not in the UV band. We consider such UV upper limits rather generous because our adopted limit on α_{ox} corresponds to quasars and AGNs that are much more luminous than the objects in our sample ($|\alpha_{ox}|$ decreases with decreasing UV luminosity; cf. Strateva et al. 2005; Steffen et al. 2006).[6]

In an effort to recover the intrinsic luminosities of the AGNs we corrected their UV and X-ray fluxes for extinction. In the X-ray band, extinction corrections are more reliable than in the UV since the column density can be determined

[6] It is noteworthy that α_{ox} may have some dependence on redshift, as argued by Kelly et al. (2007). Nevertheless, when the dependence on redshift is taken into account, the value we have adopted as an upper limit on α_{ox} still corresponds to quasars and AGNs that are much more luminous than the objects of our sample. It is also noteworthy that Tang et al. (2007) have argued that a correlation between α_{ox} and UV luminosity is not firmly established, although they do conclude that such a correlation is likely present in a complete subsample of the Steffen et al. (2006) data.

directly by fitting the observed X-ray spectrum (see details in Paper I). Extinction corrections in the UV involve a number of assumptions, and as a result they are subject to considerable uncertainty. Therefore, we have tried to err on the side of caution and overestimate the intrinsic luminosity rather than underestimating it. To obtain the total reddening toward the UV source, we used the total hydrogen column densities derived from fits of an absorbed power-law model to the X-ray spectra. We converted these to a color excess using the relation between column density and visual extinction for the Milky Way, $N_{\rm H}/A_{\rm V} = 1.79 \times 10^{21}$ cm^{-2} mag^{-1} (Predhl & Schmitt 1995), and the Seaton (1979) extinction law, which implies that $R_{\rm V} \equiv A_{\rm V}/E(B-V) = 3.2$. The resulting values of $E(B-V)$ are given in Paper I along with the corresponding values for the interstellar medium of the Milky Way in the direction of the source (taken from Schlegel et al. 1998). Comparing the two values of the color excess, we find that the value derived from the X-ray spectrum is comparable to or greater than the Milky Way value, suggesting that the former value also captures extinction in the host galaxy of the AGN. Using the color excess derived from the X-ray spectrum we computed extinction corrections for the UV data by separately applying the Milky Way extinction laws of Seaton (1979) and Caredelli et al. (1989), the Large and Small Magellanic Cloud extinction laws of Korneef & Code (1981) and Bouchet et al. (1985), respectively, and the starburst galaxy extinction law of Calzetti et al. (1994). In the end we adopted the Seaton (1979) law since this gives the largest correction. We note, however, that UV luminosities obtained with the other Milky Way or Magellanic Cloud laws are less than 10% lower than the values we have adopted. The corrected UV fluxes are included in Paper I along with a discussion of the differences between the five correction schemes (see Section 3.2 of Paper I).

3. IONIZING LUMINOSITIES AND PHOTON RATES

We evaluated the 1 Ry–100 keV ionizing luminosities ($L_{1\ \mathrm{Ry-100\ keV}}$) and ionizing photon rates ($Q_{1\ \mathrm{Ry-100\ keV}}$) of the AGNs in our sample, after extrapolating their 2–10 keV X-ray spectra, in two different ways. We First integrated the SED, assuming that pairs of points could be connected by a power law. Under this assumption, the luminosity and photon rate of each segment were computed analytically and then the contributions of different segments were summed, i.e.,

$$L_{1\ \mathrm{Ry-100\ keV}} = \sum_{i=1}^{N-1} \int_{\nu_i}^{\nu_{i+1}} L_\nu \, d\nu \quad \text{and}$$

$$Q_{1\ \mathrm{Ry-100\ keV}} = \sum_{i=1}^{N-1} \int_{\nu_i}^{\nu_{i+1}} \frac{L_\nu}{h\nu} \, d\nu. \qquad (1)$$

The upper limit of integration is appropriate because the X-ray spectra of Seyfert galaxies typically cut off at energies between 50 and 150 keV (Molina 2009).[7] The results are listed in Columns 4 and 5 of Table 1. If at least one of the measured points in an SED is an upper limit we take $L_{1\ \mathrm{Ry-100\ keV}}$ and $Q_{1\ \mathrm{Ry-100\ keV}}$ to be upper limits as well.

The above scheme relies on the assumption that the ionizing SED of the AGN is a power law between the near-UV and soft X-ray bands (typically 2500 Å to 0.5 keV), which is not necessarily correct. The SEDs of more luminous AGNs, such as Seyfert galaxies and quasars, are thought to have a significant flux in the far-UV band (see, for example, Elvis et al. 1994), which would not be observable in the case of the weak AGNs of our sample. To deal with this possibility we also evaluated the 1 Ry–100 keV ionizing luminosities and ionizing photon rates of the AGNs in our sample by assuming that their SEDs are similar to the standard radio-quiet quasar SED presented by Elvis et al. (1994). Even though the weak AGNs in LINERs are thought to be *radio-loud* (e.g., Nagar et al. 2001; Terashima & Wilson 2003; Ulvestad & Ho 2001; Anderson et al. 2004), we have opted to use the *radio-quiet* quasar template because it has a higher value of $\alpha_{\rm ox}$ than the radio-loud quasar template (1.36 versus 1.34). In other words, we are conservatively adopting the higher UV luminosity for a given X-ray luminosity. We also note that these values of $\alpha_{\rm ox}$ are higher than those of 80% of the weak AGNs in our sample, which means that by using them we are overestimating the UV luminosity and photon rate for the vast majority of these weak AGNs. The standard radio-quiet quasar SED, when normalized to a 2–10 keV X-ray luminosity of $L_{2-10\ \mathrm{keV}} = 1 \times 10^{40}$erg s^{-1}, yields an ionizing luminosity of $L_{1\ \mathrm{Ry-100\ keV}} = 9.77 \times 10^{40}$erg s^{-1} and an ionizing photon rate of $Q_{1\ \mathrm{Ry-100\ keV}} = 1.38 \times 10^{51}$erg s^{-1} after extrapolating the X-ray power-law portion to 100 keV. We obtained the ionizing luminosities and ionizing photon rates of our sample AGNs by scaling their 2–10 keV X-ray luminosities accordingly. The results are listed in Columns 6 and 7 of Table 1. In cases where we only have an upper limit to the 2–10 keV luminosity we take $L_{1\ \mathrm{Ry-100\ keV}}$ and $Q_{1\ \mathrm{Ry-100\ keV}}$ to be upper limits as well. This scheme has some advantages over the previous one: (1) it bypasses uncertainties in extinction corrections in the UV since it relies only on the X-ray extinction, which is derived by fitting the X-ray spectrum, (2) it depends only on the 2–10 keV X-ray luminosity, which is the quantity measured for most of our objects, and (3) it bypasses indirect determinations of upper limits to the UV flux through $\alpha_{\rm ox}$. On the negative side, this scheme is sensitive to the assumed shape of the SED. Theoretical models (e.g., Di Matteo et al. 2000; Ball et al. 2001; Ptak et al. 2004) suggest that the SEDs of weak AGNs in LINERs have a lower far-UV luminosity relative to the X-ray luminosity than Seyfert galaxies and quasars. On the other hand, Maoz (2007) has argued that the values of $\alpha_{\rm ox}$ of such weak AGNs are compatible with the values found among Seyfert galaxies, which suggests that the SEDs of weak AGNs in LINERs include the same number of UV photons per unit X-ray luminosity as those of Seyferts. Indeed, our study of the average SED of the little monsters in Paper I bolsters this view.

4. RESULTS: COMPARISON OF IONIZING POWER AND EMISSION-LINE POWER

To assess the energy budget of the LINERs in our sample we compare in Figure 2, the ionizing luminosities of their weak AGNs to the corresponding Hα luminosities. In Figure 2(a), we plot the ionizing luminosity obtained by integrating the AGN SED against the Hα luminosity. In order to use this plot for our goals, we need to relate the Hα luminosity of the emission-line gas to its total cooling rate, which we do by appealing to photoionization models. In particular, we use the models computed by Lewis et al. (2003), employing the photoionization code Cloudy (v94.0; see Ferland et al. 1998) and adopting a representative low-luminosity AGN SED.

[7] If we extrapolate the observed X-ray spectra to 500 keV instead, the resulting ionizing luminosity increases only by a few percent and the ionizing photon rate increases by a negligible amount.

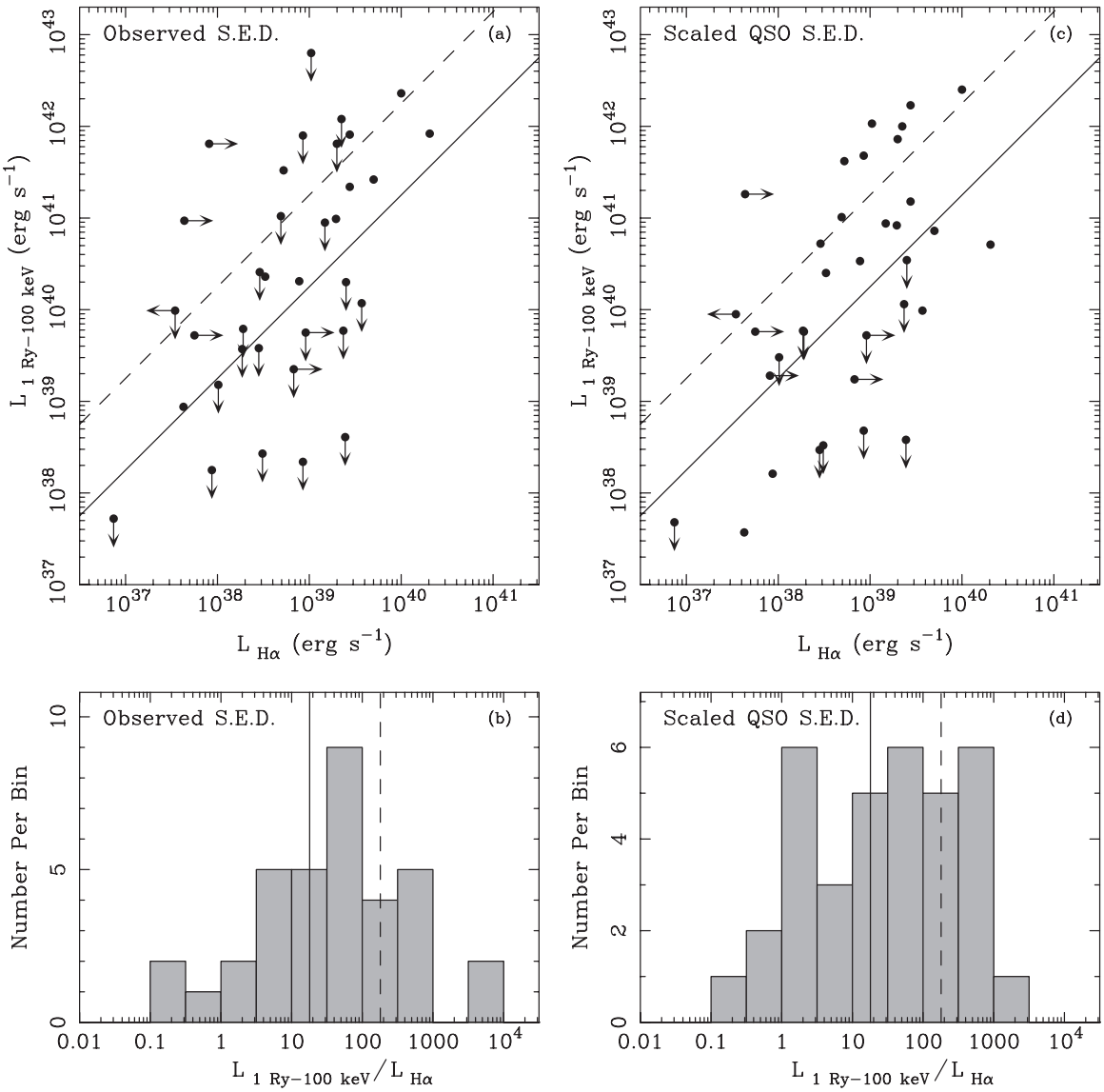

Figure 2. (a) Ionizing (1 Ry–100 keV) luminosity of LINERs in our sample, plotted against their Hα luminosity. The ionizing luminosity was determined by directly integrating the SED, as described in Section 3. Arrows denote upper limits on the ionizing luminosity. The ionizing luminosity balances the cooling rate of a uniform, photoionized slab of a given Hα luminosity along the solid line ($L_{1\ \mathrm{Ry-100\ keV}} = L_{\mathrm{cool}} = 18\ L_{\mathrm{H}\alpha}$; see Section 4 of the text). If only a fraction f_c (= 0.1) of the ionizing photons are absorbed by the nebula, then energy balance is represented by the dashed line ($L_{1\ \mathrm{Ry-100\ keV}} = L_{\mathrm{cool}}/f_c$). (b) An alternative representation of (a) in the form of a histogram of the ratio $L_{1\ \mathrm{Ry-100\ keV}}/L_{\mathrm{H}\alpha}$. The solid and dashed lines have the same meaning as in (a). (c) Same as (a) but with ionizing luminosities measured by scaling a standard quasar SED to the 2–10 keV luminosity of the AGN. (d) Same as (b) but with ionizing luminosities measured by scaling a standard quasar SED to the 2–10 keV luminosity of the AGN.

These models spanned a wide range of ionization parameters ($\log U = -4.5, -4.0, -3.5, -3.0$), densities ($\log[n/\mathrm{cm}^{-3}] = 2, 3, 4, 5, 6$), and metallicities ($Z/Z_\odot = 0.3, 1, 2$). By re-examining the results of these calculations, we find a tight relation between the total cooling rate of the nebula and its Hα luminosity, namely $\langle L_{\mathrm{cool}}/L_{\mathrm{H}\alpha}\rangle = 18$ with a dispersion of 2 about the mean. From this we conclude that energy balance in the nebula requires that $L_{1\ \mathrm{Ry-100\ keV}} > 18\ L_{\mathrm{H}\alpha}$. This condition is represented by a solid line in Figure 2(a). We note that 12/35 LINERs in our sample do not meet this most fundamental requirement. In practice, it is quite possible that only a fraction, f_c, of the ionizing luminosity of the AGN are absorbed by the line-emitting gas. This could be because the gas is not completely optically thick to the ionizing photons, because it is porous (i.e., inhomogeneous on small scales), or because it has a large-scale geometry such that it only covers a fraction of the sky, as seen from the AGN (e.g., it could be toroidal). In such a case, the condition for energy balance becomes $L_{1\ \mathrm{Ry-100\ keV}} > 18\ L_{\mathrm{H}\alpha}/f_c$. We illustrate an example of this new condition, for $f_c = 0.1$, in Figure 2(a) as a dashed line. If $f_c = 0.1$, 24/35 LINERs in our sample fail this stricter requirement. Figure 2(b) is an alternative representation of Figure 2(a) where we show the distribution of the ratio $L_{1\ \mathrm{Ry-100\ keV}}/L_{\mathrm{H}\alpha}$ (it is effectively a projection of the data along the diagonal lines in Figure 2(a)). The solid and dashed lines in Figure 2(b) have the same meaning as in Figure 2(a).

Figures 2(c) and (d) are analogous to Figures 2(a) and (b) with the difference that the ionizing luminosities and photon rates were obtained by scaling the standard quasar SED. Figure 2(c) leads to very similar conclusions as Figure 2(a); if we assume that all ionizing photons are absorbed by the emission-line nebula, then 14/35 LINERs fail the energy budget test. If

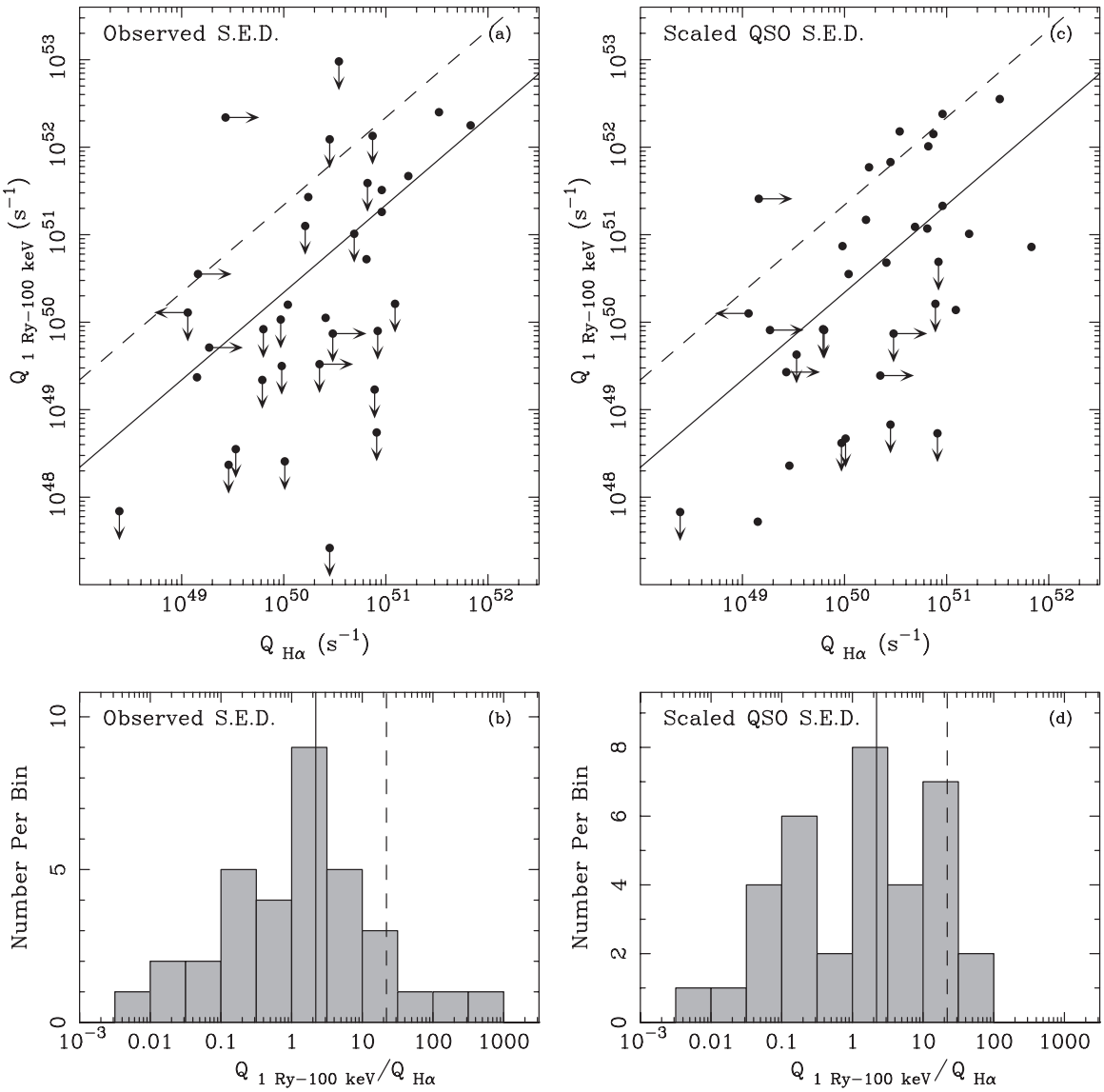

Figure 3. (a) Ionizing (1 Ry–100 keV) photon rate of LINERs in our sample, plotted against their Hα photon rate. The ionizing photon rate was determined by directly integrating the SED, as described in Section 3. Arrows denote upper limits on the ionizing photon rate. The ionizing photon rate balances the Hα photon rate along the solid line ($Q_{1\ \mathrm{Ry-100\ keV}} = 2.2\ Q_{\mathrm{H}\alpha}$; see Section 4 of the text). If only a fraction f_c (= 0.1) of the ionizing photons are absorbed by the nebula, then photon number balance is represented by the dashed line ($Q_{1\ \mathrm{Ry-100\ keV}} = 2.2\ Q_{\mathrm{H}\alpha}/f_c$). (b) An alternative representation of (a) in the form of a histogram of the ratio $Q_{1\ \mathrm{Ry-100\ keV}}/Q_{\mathrm{H}\alpha}$. The solid and dashed lines have the same meaning as in (a). (c) Same as (a) but with ionizing photon rates measured by scaling a standard quasar SED to the 2–10 keV luminosity of the AGN. (d) Same as (b) but with ionizing photon rates measured by scaling a standard quasar SED to the 2–10 keV luminosity of the AGN.

we apply the stricter condition that only 10% of the ionizing luminosity contributes to the heating of the nebula, then 24/35 LINERs appear to suffer from a deficit in their energy budgets.

A complementary test is depicted in Figure 3(a), where we compare the ionizing photon rates of the weak AGNs in our sample of LINERs to the corresponding Hα photon rates. The ionizing photon rate in this figure was obtained by direct integration of the SED. Assuming that Hα photons are produced by case B recombination, one Hα photon is emitted for every 2.2 recombinations (Osterbrock 1989). Collisional excitation of Hα is unlikely to make a significant contribution to the observed Hα photon rate since the densities in the emission-line nebulae of LINERs are thought to be relatively low. Therefore, the minimum requirement for photon balance, if all ionizing photons are absorbed by the emission-line nebula, is $Q_{1\ \mathrm{Ry-100\ keV}} > 2.2\ Q_{\mathrm{H}\alpha}$. This condition is shown as a solid line in Figure 3(a). Only 14/35 LINERs satisfy this condition. As we have argued earlier in this section, it is possible that only a fraction f_c of the ionizing photons are absorbed by the emission-line nebula. Thus, a more appropriate form of the photon balance condition is $Q_{1\ \mathrm{Ry-100\ keV}} > 2.2\ Q_{\mathrm{H}\alpha}/f_c$, which is represented in Figure 3(a) as a dashed line, for $f_c = 0.1$. This stricter requirement is satisfied by only 4/35 LINERs in our sample. Figure 3(b) is analogous to Figure 2(b); it shows the distribution of the ratio $Q_{1\ \mathrm{Ry-100\ keV}}/Q_{\mathrm{H}\alpha}$ with the solid and dashed lines having the same meaning as in Figure 3(a). Figures 3(c) and (d) show the same test as Figures 3(a) and (b), but with the ionizing photon rates determined by scaling the standard quasar SED. The conclusions from Figure 3(c) are the same as those from Figure 3(a); only 15/35 LINERs satisfy the minimum photon balance condition and only 5/35 objects satisfy the stricter condition, assuming $f_c = 0.1$.

5. SUMMARY AND DISCUSSION

The energy and photon budget tests presented in the previous section show that the weak AGNs in LINERs are unable to power the luminosity measured in the $2'' \times 4''$ spectroscopic slit by photoionization. The AGN can provide enough ionizing photons to explain the observed Hα luminosity in only 43% of the LINERs of our sample, if all the available ionizing photons are absorbed by the emission-line gas. More realistically, however, if only a fraction of the available ionizing photons are absorbed by the emission-line nebula, then only in a small minority of cases is the AGN ionizing photon rate sufficient to explain the observed Hα photon rate. In approximately 1/3 of the cases the ionizing photon rate from the AGN falls short of the required rate by an order of magnitude or more.

Our conclusion is in agreement with most of the previous studies (see Section 1), even though we have assumed a different shape for the SED. The main improvement in our approach is that we have assumed AGN SEDs that are not simple power laws. The observed SEDs that we used can be often described by a relatively steep power law from 2500 Å to 0.5 keV and a flatter power law from 0.5 to 10 keV (see, for example, Figures 2 and 7 of Paper I). Our template SEDs include a "big blue bump," also resulting in a steep slope in the extreme-UV band, which then becomes flatter in the X-ray band. In contrast, Flohic et al. (2006) extrapolated the power law from the X-ray band to lower energies and probably underestimated the ionizing luminosity by missing a substantial fraction of the UV photons. On the other hand, Maoz et al. (1995) used a power-law SED normalized to the UV flux, thus probably overestimating the ionizing luminosity.

5.1. Have We Missed Any Ionizing Photons from the Little Monster?

Before we consider other processes that contribute to the ionizing photon budget, we ask whether the ionizing luminosities and photon rates that we have determined for the AGNs in question represent the true values.

1. Could the ionizing continuum that we detect be extinguished, thus weaker than what illuminates the line-emitting gas? We consider this an unlikely possibility since we have made generous corrections for extinction and have tried to err on the side of caution. One of the methods we used to obtain the ionizing luminosity, scaling the standard quasar SED to the observed 2–10 keV luminosity, bypasses this problem. It relies only on a measurement of the X-ray flux which can be reliably corrected for extinction since the column is determined directly from the shape of the X-ray spectrum. Two additional pieces of evidence bolster this view: (a) the morphology of the emission-line regions of LINERs is rarely bipolar, disfavoring the presence of obscuring tori of the type invoked in Seyfert galaxy unification schemes (Pogge et al. 2000), and (b) if the ionizing continuum were considerably stronger than what we observe, the emission-line ratios would have been different, i.e., they would have resembled those of Seyferts galaxies, indicating a higher ionization level of the line-emitting gas.
2. Could there be an unseen far-UV "bump" in the SED which makes up the power deficit? This effect is also captured by our method of obtaining the X-ray luminosity by scaling the standard quasar SED, since the template already includes a far-UV bump. If the far-UV bump in the SED of "little monsters" were stronger than that of quasars, it would have revealed itself in the form of a larger absolute value of α_{ox} and/or a soft X-ray excess, above the high-energy power-law shape; neither of these features is observed. Moreover, a stronger far-UV bump would have also produced Seyfert-like rather than LINER-like emission-line ratios.
3. Could we be observing the "echo" of a previous epoch, a few hundred years ago, when the "little monster" was more ferocious? This possibility was considered by Eracleous et al. (1995), who showed that the reverberation of an ionizing flare in the nebula produces LINER-like emission-line ratios. However, this cannot be a universal explanation. This mechanism requires the flare recurrence times to be of order a few hundred years and the duty cycle to be relatively short (i.e., of order a few tens of percent). However, the duty cycle cannot be arbitrarily short because that would affect the diagnostic line ratios that are used to classify an object as a LINER. More specifically, the [O III] λ5007/Hβ ratio, which is often used as a diagnostic, is very sensitive to the duty cycle because of the very short decay time of the [O III] λ5007 line following the decay of the ionizing continuum. The required combination of recurrence times and duty cycles of such flares suggests that at least some of the central UV sources of LINERs should be observed to decay systematically over the course of a few decades. But this is in contradiction with the observations of Maoz et al. (2005, 1995), which show the UV sources to persist over timescales on the order of a decade. Therefore, we are led to disfavor this particular scenario based on this particular combination of duty cycle and recurrence time. We also note an additional observational test that bolsters our conclusion. The echo of an ionizing continuum flare should be detectable in a narrow-band [O III] λ5007 image in the form of a ring-like structure. But Pogge et al. (2000) have specifically looked for such structures in their emission-line imaging survey and did not find convincing evidence for them.

The "little monster" is still capable of powering the line emission from a compact region immediately surrounding it. In fact, the narrow-band images of Pogge et al. (2000) show centrally concentrated emission regions. To illustrate this point, we have collected in Table 2 measurements of the Hα luminosity of 12 objects made with the *HST* through apertures of angular sizes of a few tenths of arcseconds (after making extinction corrections). These measurements come from Space Telescope Imaging Spectrograph (STIS) spectra (Shields et al. 2007) and WFPC2 narrow-band images (Pogge et al. 2000). For another two objects, we measured the line fluxes ourselves from archival STIS and Faint Object Spectrograph (FOS) spectra. In the case of the narrow-band images, the filter includes both the Hα line as well as the [N II] doublet that straddles it. We have rescaled the flux according to the relative intensities of these lines reported by Ho et al. (1997b). Adopting the relative intensities from the large-aperture spectrum is justified by the results of Shields et al. (2007), who find that in the majority of objects in their sample, the value of the [N II]/Hα ratio measured in the narrow STIS aperture is within a factor of 1.6 of the value measured in the large-aperture spectrum of Ho et al. (1997b). In Figure 4, we plot the ionizing photon rate (from Column 7 of Table 1) against the small-aperture Hα photon rate for these 12 objects in order to assess their energy budgets following the methodology of Section 4. Examining this figure we see that in nine out of the 12 objects the ionizing photon rate is at least several times higher than the rate required to power the Hα lines. Thus, the compact

Table 2
Hα Luminosities Through Small Apertures

Galaxy (1)	$\log L_{H\alpha}$ [a] (2)	$Q_i/Q_{H\alpha}$ (3)	Aperture Size (4)	Notes (5)
NGC 0404	36.83	0.14	$R = 0\farcs23$	b
NGC 1097	38.35	46.16	$0\farcs25 \times 0\farcs2$	c
NGC 3031	38.40	18.07	$0\farcs25 \times 0\farcs2$	c
NGC 3998	40.08	5.15	$R = 0\farcs23$	b
NGC 4143	38.13	19.02	$0\farcs25 \times 0\farcs2$	d
NGC 4314	36.67	< 1.58	$0\farcs25 \times 0\farcs2$	d
NGC 4374	38.30	4.24	$R = 0\farcs23$	b
NGC 4486	38.99	3.85	$R = 0\farcs23$	b
NGC 4548	37.21	79.75	$0\farcs25 \times 0\farcs2$	d
NGC 4579	38.73	77.60	$R = 0\farcs23$	b
NGC 4594	39.29	0.93	$R = 0\farcs23$	b
NGC 5055	< 37.21	> 2.89	$0\farcs25 \times 0\farcs2$	d

Notes.
[a] The luminosities are measured in erg s^{-1}. They have been corrected for extinction using the values of $E(B-V)$ from the emission-line gas reported by Ho et al. (1997b) and the Seaton (1979) extinction law.
[b] Taken from the narrow-band imaging survey of Pogge et al. (2000). Since, the filter includes the Hα line and [N II] doublet, the flux was rescaled according to the relative strengths of the lines measured in the ground-based spectra of Ho et al. (1997b).
[c] Measured from the archival *HST* spectrum.
[d] Taken from Shields et al. (2007).

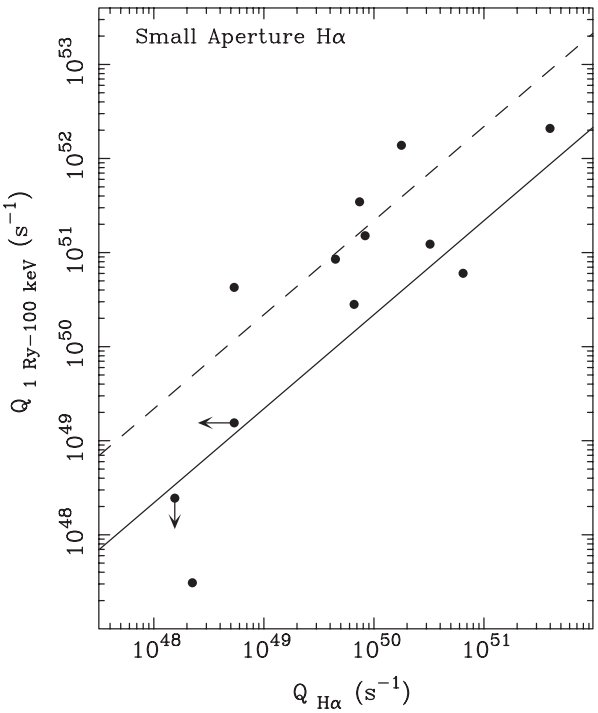

Figure 4. Ionizing (1 Ry–100 keV) photon rate of 12 of the LINERs in our sample, plotted against their Hα photon measured in a small aperture. The ionizing photon rate was determined by scaling the ionizing photon rate of the standard radio-quiet quasar SED, according to the 2–10 keV luminosity of the AGN. The Hα photon rates were either measured directly from an *HST* spectrum or determined from the ground-based spectrum by scaling according to the fluxes measured in narrow-band images (see details in Table 2 and in Section 5 of the text). Arrows denote upper limits on the ionizing photon rate or the Hα photon rate. The ionizing photon rate balances the Hα photon rate along the solid line ($Q_{1\ Ry-100\ keV} = 2.2\ Q_{H\alpha}$; see Section 4 of the text). If only a fraction f_c (= 0.1) of the ionizing photons are absorbed by the nebula, then photon number balance is represented by the dashed line ($Q_{1\ Ry-100\ keV} = 2.2\ Q_{H\alpha}/f_c$).

emission-line regions measured through the small *HST* apertures could well be powered by the "little monster." However, this test also underscores our earlier conclusion that the "little monster" can power only a small fraction of the line luminosity measured through the large, $2'' \times 4''$ aperture.

The ionizing-photon deficit that we have identified in LINERs should not extend to more luminous AGNs, even though this deficit appears even when we assume a quasar-like SED. More luminous AGNs should emit more ionizing photons per unit Hα luminosity than LINERs based on the following two indicators. (1) A close examination of Figure 7 of Flohic et al. (2006) shows that most LINERs fall below the extrapolation of the $L_{2-10\ keV}$–$L_{H\alpha}$ correlation defined by more luminous AGNs (shown in Figure 2 of Ho et al. 2001). This means that the $Q_i/Q_{H\alpha}$ ratio for more luminous AGNs will be higher than that of the weak AGNs in LINERs. (2) For luminous AGNs with $(\nu L_\nu)_{2500\ Å} \gtrsim 10^{43}$ erg s^{-1} the values of α_{ox} are higher than those of the weak AGNs in LINERs (see Figure 2 of Maoz 2007). This implies that luminous AGNs emit more ionizing photons per unit X-ray luminosity than the weak AGNs in LINERs.

5.2. Alternative Sources of Power

Thus, we are led to seek other power sources that could make up the power deficit in LINERs. These power sources fall in two broad categories, sources of ionizing radiation that are not associated with the "little monster" and sources of mechanical heating, which may or may not be associated with the "little monster." Suitable power sources must fulfill two conditions: (1) they must be able to provide the requisite power (at least in principle), and (2) they must lead to LINER-like emission-line ratios.

1. *Mechanical Power Delivered by Compact Jets.* A number of authors have shown that the "little monsters" found in LINERs are associated with radio sources with a high brightness temperature and/or elongated radio morphology (e.g., Nagar et al. 2001, 2005; Ulvestad & Ho 2001; Anderson et al. 2004; Filho et al. 2004). This has been interpreted as evidence for jets, which give rise to the bulk of the observed radio emission. Nagar et al. (2005) have estimated that the kinetic luminosity of the jets can exceed the 2–10 keV X-ray luminosity by as much as 4.5 orders of magnitude. More specifically, in half of the weak AGNs in the sample of Nagar et al. (2005) the kinetic power of the jet exceeds the 2–10 keV X-ray luminosity by at least a factor of 30. In comparison, the ionizing luminosity of the "little monsters" in our sample is 5–10 times larger than their 2–10 keV luminosity.[8] Thus, the kinetic power of the jets can be up to three orders of magnitude higher than the ionizing luminosity of the AGN. Even if only a small fraction of this power can be used to energize the emission-line nebula through shocks, it would be enough to balance the energy budget.

   Shock excitation models have had mixed success in explaining the emission-line spectra of LINERs. On the positive side, Nicholson et al. (1998) find that the optical+UV spectrum from the nucleus of NGC 3998 can be explained by models invoking slow shocks ($\lesssim$150 km s^{-1}; see Shull & McKee 1979). On the negative side, however, Ho et al.

[8] The standard radio-quiet quasar SED gives $L_{1\ Ry-100\ keV}/L_{2-10\ keV} = 10$. Integrating the observed SEDs of the 10 objects in our sample which are detected both in the X-rays and the UV and the UV light is *not* dominated by hot stars (see Paper I), we obtain a mean value of this ratio of 5, a geometric mean of 6, and a median of 9.

(1996) have shown that the optical+UV spectrum of the nucleus of M81 is not compatible with shock models. More generally, Maoz et al. (1998) pointed out that none of the UV spectra of the seven LINERs in their sample resembles those predicted by shock models (they either have broad, AGN-like emission lines or they resemble the spectra of starbursts, lacking strong emission lines). This is also the case for the nuclear UV spectrum of NGC 1097 (Storchi-Bergmann et al. 2005).

Perhaps the role of shocks can be better understood by considering the case studies of the nucleus and circumnuclear disk of M87 based on spectra obtained through small (subarcsecond) apertures with the *HST*. According to Dopita & Sutherland (1996) and Dopita et al. (1997), the optical+UV emission-line spectrum of the circumnuclear gaseous disk of M87 can be explained by models invoking fast ($\gtrsim$200 km s^{-1}) shocks. After studying the inner regions of the disk of M87, Sabra et al. (2003) conclude that the gas is excited by photons from the active nucleus but they also note that there appears to be a transition from photoionization to shock excitation at a distance of a few tens of parsec from the center.

2. *Photoionization by Young Stars.* Young star clusters are found in some LINERs, although they are not very common. For example, Maoz et al. (1998) find the signature of hot stars in the UV spectra of 3/7 LINERs in their sample (NGC 404, NGC 5055, and NGC 4569), while by similar means, Storchi-Bergmann et al. (2005) find a compact (<9 pc) star-forming region around the AGN in NGC 1097. We can make rough estimates of the incidence of young stellar populations in the nuclei of LINERs by consulting the results of Cid Fernandes et al. (2005) and González Delgado et al. (2004) who have used spectral decomposition techniques to study the optical and UV spectra of LINERs and "transition objects." Based on these considerations, we find that ∼10%–15% of LINERs harbor young stellar populations in their nuclei.

   When present, young star clusters may be able to provide enough power to balance the energy budget. In fact, Maoz et al. (1998) have demonstrated that this is possible for the three LINERs with starburst-like UV spectra out of their sample of seven. They used synthetic spectra of young star clusters normalized to the observed UV luminosities to show that there are enough ionizing photons in the unobservable far-UV band to account for the observed emission-line luminosities (assuming that all ionizing photons are absorbed by the emission-line nebula). We also note that photoionization by extremely hot, massive stars can explain the relative intensities of the optical emission lines, as shown by the models of Terlevich & Melnick (1985), Filippenko & Terlevich (1992), Shields (1992), and Barth & Shields (2000). In addition to photoionization, shocks from supernovae or stellar winds in a young cluster could also contribute to the excitation of the emission-line gas.

3. *Photoionization by Post-AGB Stars from an Old or Intermediate-age Stellar Population.* This idea was suggested by Binette et al. (1994) to explain the line emission from normal elliptical galaxies, but the authors also noted that the same scenario may be applicable to LINERs. A variant of this idea, in which the ionizing photons are provided by the central stars of planetary nebulae was explored by Taniguchi et al. (2000). Using a population synthesis simulation, Binette et al. (1994) computed the evolution of the ionizing photon rate from an aging stellar population and found that at late times (after the demise of the hot, massive stars at $t \gtrsim 10^8$ years) the dominant contribution to the ionizing luminosity comes from post-AGB stars. They also found that the ionizing photon rate at late times declines fairly slowly with time (it drops by an order of magnitude or less between the ages of 10^8 and 10^{10} years). By carrying out a series of photoionization calculations, they demonstrated that the resulting emission-line spectra resemble those observed in LINERs. This scenario is attractive because it relies only on ionizing photons from the old stellar population. It is also bolstered by one of the results of the X-ray survey of LINERs by Flohic et al. (2006): the Hα luminosity is more tightly correlated to the soft (0.5–2 keV) than to the hard (2–10 keV) X-ray luminosity of the nucleus, which is likely to be associated with stellar processes (e.g., stellar winds).

   To investigate the plausibility of this scenario, we have used the surface brightness profiles of eight elliptical or S0 galaxies from our sample available in the literature. These objects, listed in Table 3, were observed in bands resembling the Johnson *V* or *B* bands with the *HST*'s WFPC, WFPC2, or Advanced Camera for Surveys (ACS). Thus, we are able to estimate whether there are enough post-AGB stars within the $2'' \times 4''$ aperture of the spectroscopic observations (Ho et al. 1995) to provide the requisite number of ionizing photons. After integrating the surface brightness over the area of the spectroscopic aperture and applying the appropriate color corrections (see details in Table 3 and associated footnotes) we derived the slit *B* magnitudes. The population synthesis model of Binette et al. (1994) gives a mass-to-light ratio of $M/L_{\rm B} = 8(M/L_{\rm B})_{\odot}$ and a specific ionizing photon rate from post-AGB stars of $dQ_{\star}/dM = 7.3 \times 10^{40}$ s^{-1} $M_{\odot}^{-1}$, allowing us to estimate the total ionizing photon rates from post-AGB stars within the spectroscopic aperture, $Q_{\star,\mu_{\rm B}}$ (where the subscript $\mu_{\rm B}$ indicates that $Q_{\star}$ was obtained from the galaxy's surface brightness profile). We summarize our results in Table 3, where we also compare $Q_{\star,\mu_{\rm B}}$ to the Hα photon rate, $Q_{\rm H\alpha}$, and the ionizing photon rate from the "little monster," $Q_{\rm AGN}$.

   An alternative way of obtaining $Q_{\star}$ (used by Ho 2008) employs the spectroscopic *B* magnitude, m_{44}, measured and reported by Ho et al. (1997b). After transforming m_{44} to a standard *B* magnitude via $m_{\rm B} = m_{44} + 0.140$,[9] we apply the procedure of the previous paragraph. We denote the ionizing photon rate obtained in this manner as $Q_{\star,m_{44}}$ and we include the resulting values in Table 1 for the galaxies for which m_{44} is available. The method involving m_{44} is subject to the uncertainty that the *B* magnitude is not measured in a standard manner. Therefore, we have compared the resulting values of $Q_{\star,m_{44}}$ and $Q_{\star,\mu_{\rm B}}$ for all the objects of Table 3 and we have found that the ratio $Q_{\star,m_{44}}/Q_{\star,\mu_{\rm B}}$ has a mean value of 1 and a standard deviation of 0.6, indicating that the agreement between the two methods is reasonably good.

   An examination of Table 3 shows that in 2/8 cases the old stellar population provides enough ionizing photons to

[9] The slit magnitude is defined as $m_{44} = -2.5 \log f_{\nu} - 48.6$ and it is determined from the spectra by averaging the flux density in two narrow windows straddling 4300 Å: 4262–4281 Å and 4360–4375 Å (Ho et al. 1997b). In comparison, the standard *B* magnitude has a bandpass with an effective wavelength of 4300 Å and it is defined such that $m_{\rm B} = -2.5 \log(f_{\nu}/4130\ {\rm Jy})$.

Table 3
Ionizing Photons from Post-AGB Stars

Galaxy (1)	$B-V$[a] (mag) (2)	B_{slit}[b] (mag) (3)	$\log(M_\star/M_\odot)$[c] (4)	$\log Q_{\star,\mu_B}$[d] (5)	$Q_{\star,\mu_B}/Q_{H\alpha}$[e] (6)	$Q_{\star,\mu_B}/Q_{AGN}$[f] (7)	Refs.[g] (8)
NGC 3379	0.98	13.81	9.64	50.50	11.02	234	1
NGC 3607	0.96	14.50	9.37	50.24	0.61	< 1.7	1
NGC 3608	0.98	14.82	9.24	50.10	2.00	< 2.7	1
NGC 4278	0.97	14.63	9.31	50.18	0.31	0.2	1
NGC 4374	0.99	14.96	9.35	50.22	0.65	0.6	2
NGC 4494	0.91	14.73	9.30	50.16	12.64	2.1	1
NGC 4552	0.98	14.29	9.45	50.31	1.87	1.0	1
NGC 4636	0.95	15.16	9.11	49.97	1.53	1.9	3

Notes.
[a] The $B-V$ color of the galaxy, taken from the RC3 catalog (de Vaucouleurs et al. 1991).
[b] The apparent B magnitude of the area of the galaxy within the $2'' \times 4''$ spectroscopic aperture. For NGC 4374, we integrated the g-band surface brightness profile and converted to a B magnitude using the transformation $B = g + 0.47(B-V) + 0.07$ (Smith et al. 2002). For all other galaxies we integrated the V-band surface brightness profiles and converted to a B magnitude using the colors reported in this table.
[c] The mass of stars within the area of the slit, estimated from the B-band mass-to-light ratio derived by Binette et al. (1994), $M/L_B = 8(M/L_B)_\odot$. We adopted the distances given by Ho et al. (1997b) so as to compare directly with the Hα luminosity.
[d] The ionizing photon rate of the post-AGB stars from the old stellar population ($t \sim 10^{10}$ years) in s^{-1}, estimated from the prescription of Binette et al. (1994). See details and discussion in Section 5 of the text.
[e] The ratio of the ionizing photon rate from the post-AGB stars to the Hα photon rate. If all ionizing photons are absorbed by the line-emitting gas, a minimum ratio of 2.2 is needed if the Hα photons are to be produced by case B recombination.
[f] The ratio of the ionizing photon rate from the old stellar population to the ionizing photon rate from the "little monster."
[g] References to surface brightness measurements: (1) Lauer et al. (2005), V-band light profiles from *HST*/WFPC2 F555W images; (2) Ferrarese et al. (2006), g-band light profiles from *HST*/ACS F475W images; (3) Lauer et al. (1995) V-band light profiles from *HST*/WFPC F555W images.

power the observed Hα emission, even if ~20% of these photons are absorbed by the gas. In 3/8 cases, the Hα emission could be powered by ionization from the old stellar population only if all the ionizing photons were absorbed by the gas, while in the remaining 3/8 cases, the rate of ionizing photons provided by the old stellar population falls short of the requisite rate by a factor of a few. A consideration of the values of $Q_{\star,m_{44}}$ listed in Table 1 leads to similar conclusions. In Figure 5, we show a histogram of the ratio $Q_{\star,m_{44}}/Q_{H\alpha}$ to illustrate this result. In 4/28 objects, the post-AGB stars provide enough ionizing photons to account for the observed Hα luminosity, in 5/28 objects the Hα luminosity may be powered if all the ionizing photons from the post-AGB stars are absorbed by the emission-line gas, and in the remaining 19/28 objects, the ionizing photons from the post-AGB stars cannot produce the observed Hα luminosity.

It is possible that the available ionizing photon rate is higher than what we have estimated if an intermediate-age population is present. The spectroscopic decomposition analysis of Cid Fernandes et al. (2005) and González Delgado et al. (2004) suggest that in ~30% of LINERs and "transition objects" a significant fraction of the optical and/or UV light comes from a population of intermediate age ($t \sim 10^8$–10^9 years). In such a case, the ionizing photon rates from post-AGB stars can be up to an order of magnitude higher than the values listed in Tables 1 and 3 and they would be enough to power the observed Hα luminosities in a large fraction of LINERs.

We also note that in the majority of galaxies of Table 3 the ionizing photon rates from the old stellar population exceed the ionizing photon rates from the respective AGNs. Similarly, in 14/29 galaxies in Table 1, $Q_{\star,m_{44}}/Q_i > 1$ (using the value of Q_i determined by scaling the radio-quiet quasar SED). This suggests that the old or intermediate-age stellar population can at least be as important a source of power for the emission lines as the AGN itself.

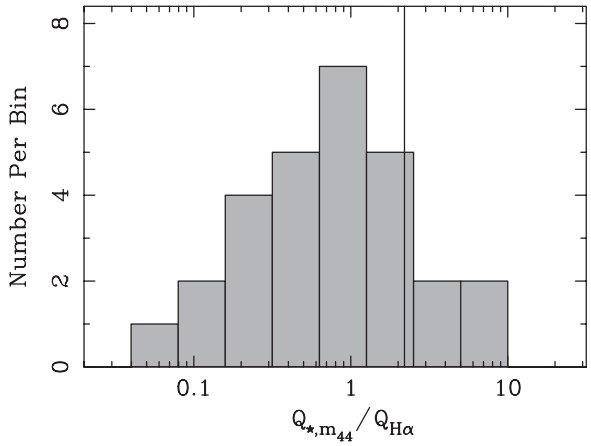

Figure 5. Distribution of the ratio of rates of ionizing photons from post-AGB stars to Hα photons in the $2'' \times 4''$ spectroscopic aperture. The rate of ionizing photons was computed from m_{44}, the spectroscopic B magnitudes reported by Ho et al. (1997b), using the methodology described in Section 5 of the text. The vertical line indicates $Q_{\star,m_{44}}/Q_{H\alpha} = 2.2$, the minimum requirement for photoionization by post-AGB stars to power the observed Hα luminosity.

5.3. Conclusions

The above considerations lead us to conclude that mechanical heating from the AGN and/or photoionization from the *old* stellar population are important power sources in a large fraction of LINERs on scales of order 200 pc from the nucleus (corresponding to the $2'' \times 4''$ aperture at the typical distances of our targets), although they may not be universal. Photoionization from the AGN can power the emission from gas on scales of order a few tens of parsec but it seems to be an inadequate source of power for gas on larger scales in the majority of cases. Young

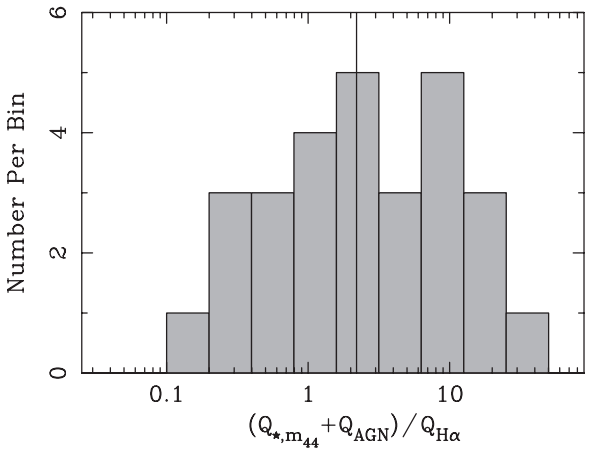

Figure 6. Distribution of the ratio of rates of ionizing photons from the AGN *plus* post-AGB stars to Hα photons in the $2'' \times 4''$ spectroscopic aperture. The rate of ionizing photons from post-AGB stars was computed from m_{44}, the spectroscopic B magnitudes reported by Ho et al. (1997b), using the methodology described in Section 5 of the text. The rate of ionizing photons from the AGN was computed by scaling the average radio-quiet quasar SED. The vertical line indicates $(Q_{\star,m_{44}} + Q_{\rm AGN})/Q_{\rm H\alpha} = 2.2$, the minimum requirement for photoionization to power the observed Hα luminosity.

stellar populations seem to be rare but important when present. Our conclusions regarding the importance of post-AGB stars are in agreement with the conclusions of Stasińska et al. (2008) who study the stellar populations and excitation mechanisms of the gas in a large sample LINERs selected from the Sloan Digital Sky Survey. The emission-line fluxes for that study were measured through an aperture of the same area as the fluxes that we have used here. Furthermore, Sarzi et al. (2010) have pursued the question of the power source of the nebular emission in the nuclei of elliptical and lenticular galaxies (on angular scales from a few to 15 arcsec), using data from the SAURON project, and have concluded that post-AGB stars are the most promising possibility. On the negative side, however, as noted by Sarzi et al. (2010), it is not clear whether population synthesis models provide reliable estimates of the numbers of post-AGB stars in an old stellar population. This is underscored by the recent UV imaging survey of M32 by Brown et al. (2008), who find considerably fewer post-AGB stars than expected. In conclusion, it appears likely that we are observing hybrid emission-line spectra powered by a combination of physical processes, with different processes potentially dominating on different scales. A similar conclusion was reached by Sabra et al. (2003) in their case study of M87.

Nevertheless, we have yet to balance the energy budget of a significant fraction of LINERs; thus we cannot uniquely identify the mechanisms that give rise to the classic LINER spectrum on scales of order a few hundred parsec around the nucleus. To illustrate this point, we compare the number of ionizing photons contributed by the combination of the AGN and the old stellar population with the number of emitted Hα photons. In Figure 6, we plot the distribution of the ratio $(Q_{\star,m_{44}} + Q_{\rm AGN})/Q_{\rm H\alpha}$ and we mark the value of 2.2, which is the minimum requirement for a balanced photon budget. As Figure 6 shows, there is a deficit of ionizing in approximately half of the targets, even if we add the contributions from the AGN and the post-AGB stars. This suggests that there is at least one important power source that remains unidentified.

Perhaps the most direct way to address the question of the power source of LINERs is optical+UV spectroscopy at high spatial resolution. The 1200–3200 Å UV band is desirable because it includes important diagnostic emission lines that can distinguish between shocks and photoionization. It is also the best band to search for the signature of massive stars. High spatial resolution is desirable in order to map out the nuclear region spectroscopically and investigate whether different mechanisms are responsible for exciting the emission-line gas at different distances from the center. With such UV spectra it may be possible to assess the role of shocks in powering the emission-line regions on scales of order a few hundred parsec by comparing the relative intensities of weak optical and UV lines with the predictions of shock models (see, for example, Dopita & Sutherland 1996; Wilson & Raymond 1999). Moreover, the photoionizing shock models of Dopita & Sutherland (1996) imply that there should be a diffuse source of ionizing continuum embedded in the line-emitting gas on scales of order a few hundred parsec, which may be detectable.

We thank the referee, D. Maoz for many helpful comments and E. C. Moran for a critical reading of the manuscript. We also thank R. A. Wade and R. B. Ciardullo for very illuminating discussions. This work was partially supported by the National Aeronautics and Space Administration through *Chandra* award number AR4-5010A issued by the *Chandra* X-Ray Observatory Center, which is operated by the Smithsonian Astrophysical Observatory for and on behalf of the National Aeronautics and Space Administration under contract NAS8-03060. M.E. acknowledges partial support from the Theoretical Astrophysics Visitors' Fund at Northwestern University and thanks the members of the group for their warm hospitality during his stay. This research has made extensive use of the NASA/IPAC Extragalactic Database (NED) which is operated by the Jet Propulsion Laboratory, California Institute of Technology, under contract with the National Aeronautics and Space Administration.

REFERENCES

Anderson, J. M., Ulvestad, J. S., & Ho, L. C. 2004, ApJ, 603, 42
Ball, G. H., Narayan, R., & Quataert, E. 2001, ApJ, 552, 221
Barth, A. J., Ho, L. C., Filippenko, A. V., & Sargent, W. L. W. 1998, ApJ, 496, 133
Barth, A. J., & Shields, J. C. 2000, PASP, 112, 753
Binette, L., Magris, C. G., Stasinska, G., & Bruzual, A. G. 1994, A&A, 292, 13
Bouchet, P., Lequeux, J., Maurice, E., Prevot, L., & Prevot-Burnichon, M. L. 1985, A&A, 149, 330
Brown, T. M., et al. 2008, ApJ, 685, L121
Calzetti, D., Kinney, A. L., & Storchi-Bergmann, T. 1994, ApJ, 429, 582
Cardelli, J. A., Clayton, G. C., & Mathis, J. S. 1989, ApJ, 345, 245
Cid Fernandes, R., González Delgado, R. M., Storchi-Bergmann, T., Pires Martins, L., & Schmitt, H. 2005, MNRAS, 356, 270
de Vaucouleurs, G., de Vaucouleurs, A., Corwin, H. G., Jr., Buta, R. J., Paturel, G., & Fouque, P. 1991, Third Reference Catalogue of Bright Galaxies, Version 3.9
Di Matteo, T., Quatart, E., Allen, S., Narayan, R., & Fabian, A. 2000, MNRAS, 311, 507
Dopita, M. A., Koratkar, A. P., Allen, M. G., Tsvetanov, Z. I., Ford, H. C., Bicknell, G. V., & Sutherland, R. S. 1997, ApJ, 490, 202
Dopita, M. A., Koratkar, A. P., Evans, I. N., Allen, M., Bicknell, G. V., Sutherland, R. S., Hawley, J. F., & Sadler, E. 1996, in ASP Conf. Ser. 103, The Physics of LINERs in View of Recent Observations, ed. Eracleous M., A. Koratkar, C. Leitherer, & L. Ho (San Francisco, CA: ASP), 44
Dopita, M. A., & Sutherland, R. S. 1996, ApJS, 102, 161
Dudik, R. P., Satyapal, S., Gliozzi, M., & Sambruna, R. M. 2005, ApJ, 620, 113
Elvis, M., et al. 1994, ApJS, 95, 1
Eracleous, M., Hwang, J. A., & Flohic, H. M. L. G. 2010, ApJS, in press (Paper I)
Eracleous, M., Livio, M., & Binette, L. 1995, ApJ, 445, L1
Ferland, G. J., Korista, K. T., Verner, D. A., Ferguson, J. W., Kingdon, J. B., & Verner, E. M. 1998, PASP, 110, 761

Ferland, G. J., & Netzer, H. 1983, ApJ, 264, 105
Ferrarese, L., et al. 2006, ApJS, 164, 334
Filho, M. E., Barthel, P. D., & Ho, L. C. 2006, A&A, 451, 71
Filho, M. E., Fraternali, F., Markoff, S., Nagar, N. M., Barthel, P. D., Ho, L. C., & Yuan, F. 2004, A&A, 418, 429
Filippenko, A. V., & Terlevich, R. 1992, ApJ, 397, L79
Flohic, H. M. L. G., Eracleous, M., Chartas, G., Shields, J. C., & Moran, E. C. 2006, ApJ, 647, 140
González Delgado, R. M., Cid Fernandes, R., Pérez, E., Martins, L. P., Storchi-Bergmann, T., Schmitt, H., Heckman, T., & Leitherer, C. 2004, ApJ, 605, 127
González-Martín, O., Masegosa, J., Márquez, I., Guerrero, M. A., & Dultzin-Hacyan, D. 2006, A&A, 460, 45
Halpern, J. P., & Steiner, J. E. 1983, ApJ, 269, L37
Heckman, T. M 1980, A&A, 87, 152
Ho, L. C. 2008, ARA&A, 46, 475
Ho, L. C., Filippenko, A. V., & Sargent, W. L. W. 1993, ApJ, 417, 63
Ho, L. C., Filippenko, A. V., & Sargent, W. L. W. 1995, ApJS, 98, 477
Ho, L. C., Filippenko, A. V., & Sargent, W. L. W. 1996, ApJ, 462, 183
Ho, L. C., Filippenko, A. V., & Sargent, W. L. W. 1997a, ApJ, 487, 568
Ho, L. C., Filippenko, A. V., & Sargent, W. L. W. 1997b, ApJS, 112, 315
Ho, L. C., et al. 2001, ApJ, 549, L61
Kelly, B. C., Bechtold, J., Siemiginowska, A., Aldcroft, T., & Sobolewska, M. 2007, ApJ, 657, 116
Korneef, J., & Code, A. 1981, ApJ, 247, 860
Lauer, T. R., et al. 1995, AJ, 110, 2622
Lauer, T. R., et al. 2005, AJ, 129, 2138
Lewis, K. T., Eracleous, M., & Sambruna, R. M. 2003, ApJ, 593, 115
Maoz, D. 2007, MNRAS, 377, 1696
Maoz, D., Filippenko, A. V., Ho, L. C., Rix, H.-W., Bahcall, J. N., Schneider, D. P., & Macchetto, F. D. 1995, ApJ, 440, 91
Maoz, D., Koratkar, A., Shields, J. C., Ho, L. C., Filippenko, A. V., & Sternberg, A. 1998, AJ, 116, 55
Maoz, D., Nagar, N. M., Falcke, H., & Wilson, A. S. 2005, ApJ, 625, 699
Molina, M., et al. 2009, MNRAS, 399, 1293
Nagar, N. M., Falcke, H., & Wilson, A. S. 2005, A&A, 435, 531
Nagar, N. M., Falcke, H., Wilson, A. S., & Ulvestad, J. S. 2002, A&A, 392, 53
Nagar, N. M., Wilson, A. S., & Falcke, H. 2001, ApJ, 559, L87
Nicholson, K. L., Reichert, G. A., Mason, K. O., Puchnarewicz, E. M., Ho, L. C., Shields, J. C., & Filippenko, A. V. 1998, MNRAS, 300, 893
Osterbrock, D. E. 1989, Astrophysics of Gaseous Nebulae and active Galactic Nuclei (Mill Valley: Univ. Science Books)
Phillips, M. M., Jenkins, C. R., Dopita, M. A., Sadler, E. M., & Binette, L. 1986, AJ, 91, 1062
Phillips, M. M., Pagel, B. E. J., Edmunds, M. G., & Diaz, A. 1984, MNRAS, 210, 701
Pogge, R. W., Maoz, D., Ho, L. C., & Eracleous, M. 2000, ApJ, 532, 323
Predhl, P., & Schmitt, J. H. M. M. 1995, A&A, 293, 889
Ptak, A., Terashima, Y., Ho, L. C., & Quataert, E. 2004, ApJ, 606, 173
Schlegel, D. J., Finkbeiner, D. P., & Davis, M. 1998, ApJ, 500, 525
Sabra, B. M., Shields, J. C., Ho, L. C., Barth, A. J., & Filippenko, A. V. 2003, ApJ, 584, 164
Sarzi, M., et al. 2010, MNRAS, in press (arXiv:0912.0275S)
Seaton, M. J. 1979, MNRAS, 187, 83P
Shields, J. C. 1992, ApJ, 399, L27
Shields, J. C., et al. 2007, ApJ, 654, 125
Shull, J. M., & McKee, C. F. 1979, ApJ, 227, 131
Smith, J. A., et al. 2002, PASP, 117, 1049
Stasińska, G., et al. 2008, MNRAS, 391, L29
Steffen, A. T., Strateva, I., Brandt, W. N., Alexander, D. M., Koekemoer, A. M., Lehmer, B. D., Schneider, D. P., & Vignali, C. 2006, AJ, 131, 2826
Storchi-Bergmann, T., Baldwin, J. A., & Wilson, A. S. 1993, ApJ, 410, L11
Storchi-Bergmann, T., Nemmen, R. S., Spinelli, P. F., Eracleous, M., Wilson, A. S., Filippenko, A. V., & Livio, M. 2005, ApJ, 624, L13
Strateva, I. V., Brandt, W. N., Schneider, D. P., Vanden Berk, D. G., & Vignali, C. 2005, AJ, 130, 387
Tang, S. M., Zhang, S. N., & Hopkins, P. F. 2007, MNRAS, 377, 1113
Taniguchi, Y., Shioya, Y., & Murayama, T. 2000, AJ, 120, 1265
Terashima, Y., & Wilson, A. S. 2003, ApJ, 583, 145
Terlevich, R., & Melnick, J. 1985, MNRAS, 213, 841
Ulvestad, J. S., & Ho, L. C. 2001, ApJ, 562, L133
Wilson, A. S., & Raymond, J. C. 1999, ApJ, 513, L115